

# Two-dimensional pressure measurements with nanosecond time resolution

J. Boneberg\*, S. Briaudeau\*\*, Z. Demirplak, V. Dobler, P. Leiderer

Universität Konstanz, 78457 Konstanz, Germany  
 (Fax: +49-7531/883-127, E-mail: johannes.boneberg@uni-konstanz.de)

Received: 21 July 1999/Accepted: 16 September 1999/Published online: 28 December 1999

**Abstract.** An optical setup for the measurement of acoustic shock waves is demonstrated experimentally. This sensor, which is based on surface plasmon excitation, provides ns time resolution as well as  $\mu\text{m}$  lateral resolution. Initial experiments with laser-induced plasma generation in a water cell already show that in a simple geometry high lateral resolution gives new insight into the ongoing processes.

**PACS:** 43.58.-e

Although acoustic probe techniques and shock wave generation are well known in water, acoustic transducers only permit the deduction of the time dependence of the pressure induced by the shock waves with a limited time resolution (around 10 ns) [1]. The usual acoustic measurement techniques with high time resolution [2, 3] are only able to measure space-averaged shock wave amplitudes, although it may happen that at a certain time the local pressure amplitudes are very high and can thus exceed the material damage threshold.

To our knowledge there is still no technique that is able to probe both the lateral pressure distribution and the time evolution of a shock wave simultaneously, although such a technique would have many potential applications in acoustics as well as in laser cleaning [4], laser ablation, and medicine [5]. For example in the context of laser ablation such a technique would allow the characterization of shock wave-induced local pressure. In shock wave medical applications (lithotripsy for urinary stone fragmentation, for example) one needs such a technique to avoid unwanted tissue damage due to high local pressures.

Such an acoustic probe technique (with both spatial and temporal pressure resolution) would suppose the following requirements. The rise time of a shock wave in water may be very short: values of about 10 ns are shorter than the acoustic transducers' response time. An optical probe method, however, would be suitable for this purpose [6, 7]. There, the time

resolution is limited only by the response time of the optical detector and by the transit time of the acoustic wave through the detection area which imposes a spatially localized probe technique. Such requirements are naturally fulfilled by optically excited surface waves.

## 1 Measurement principle

The surface waves used to probe the pressure variations are the so-called surface plasmon waves, which in our case are optically excited in the Kretschmann [8] configuration (Fig. 1): the excitation is provided by the evanescent electric field created by total internal reflection of a laser beam on a glass prism on which a metal film was previously evaporated. Because of their dispersion relation the surface plasmons can only be excited at a specific resonance angle  $\theta_0$  for a given optical wavelength ( $\lambda_{\text{optical}}$ ). Around this resonance angle the reflection of the exciting laser beam on the prism drops from 80% out of resonance to 0% at the center of resonance (Fig. 2). This resonance angle is very sensitive to even tiny changes of the refractive index  $n$  of the medium in which the plasmons are traveling. Thus at any fixed angle inside the resonance a change of refractive index  $\delta n$  of the external medium leads to a change of reflectivity  $\delta R$  (Fig. 2). These measurements use the pressure dependence of the refractive index of the medium  $n(P)$  to determine the amplitude

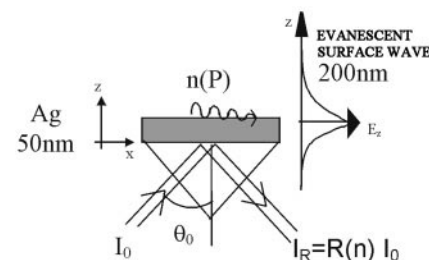


**Fig. 1.** Surface plasmon setup in the Kretschmann configuration. The evanescent wave (decay length about 200 nm) propagates at the Ag film surface ( $\approx 50$  nm thickness). It is optically excited with total internal reflection of a laser beam through a prism on which the metal film is evaporated. The laser reflectivity  $R(n)$  depends on pressure  $P$  via the external medium index of refraction  $n(P)$

\*Corresponding author.

\*\*Postdoctoral student in the framework of the TMR ERB FMRXCT089-0188 (LASER CLEANING)

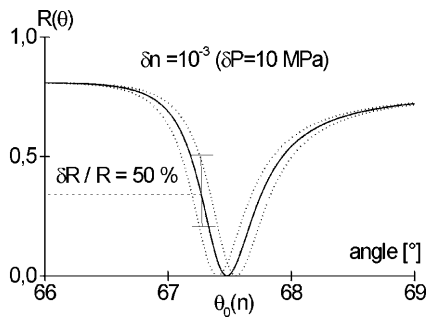


**Fig. 2.** Calculated surface plasmon resonance shape and dependence with external medium index of refraction. The Ag film is 53 nm thick evaporated on a BK7 substrate ( $n = 1.5$ ). The external medium is water ( $n = 1.33$ ). The *solid curve* is calculated for  $n = n_0 = 1.33$ . The *two dotted curves* are calculated for  $n = n_0 \pm 10^{-3}n_0$  ( $\delta n/n = 10^{-3}$ ). This small index of refraction modulation is equivalent to pressure variation  $\delta P = 10$  MPa at atmospheric static pressure

of the shock waves. The liquid chosen here is water, as it is very similar to human tissue and the change of its refractive index with pressure  $n(P)$  is well known [9].

The surface plasmons are evanescent waves. Their vertical decay length is of the order of half the excitation wavelength, which is sufficiently small to provide a transit time ( $\tau = L/v$ ) of the acoustic wave in the evanescent field smaller than 1 ns (under a static pressure of 1 atm = 0.1 MPa the acoustic velocity in water is  $v = 1500$  m/s). This transit time imposes the time resolution of this technique. The spatial resolution of the lateral pressure distribution pictures is limited by the lateral decay length of the surface plasmon wave [10]. For a perfectly smooth surface (corrugation under 1 nm) it is about 100  $\mu\text{m}$ . For a real rough surface this decay length is smaller as will be shown in the spatial resolution of the pressure lateral distribution obtained experimentally. The pressure sensitivity of this technique is related to the external medium index of refraction dependence with pressure  $n(P)$  and to the dependence of the surface plasmon resonance angle  $\theta_0(n)$  with the index of refraction of the external medium. As the plasmon resonance shape is almost Lorentzian-like and as  $n(P)$  and  $\theta(n)$  are linear functions, the reflectivity modulation is proportional to the pressure modulation with the following coefficient:

$$\alpha = (\partial R/\partial P) = \pm(\Delta\theta_{1/2})^{-1} \times (\partial\theta/\partial n) \times (\partial n/\partial P) \quad (\text{with } \Delta\theta_{1/2} \text{ the resonance full width at half maximum}).$$

For a 53 nm Ag film on BK7 glass and water at atmospheric pressure one has  $\partial R/\partial P = 2\%/MPa$  (in these conditions  $\Delta\theta_{1/2} = 0.5^\circ$ ;  $\partial\theta/\partial n = 50^\circ$ ;  $\partial n/\partial P = 2 \times 10^{-4}/MPa$  [9]). If the pressure variation is equal to 10 MPa, the calculated reflectivity change is about  $\Delta R/R \approx 50\%$  (at half maximum of the surface plasmon resonance; see Fig. 2).

## 2 Experimental setup

The pressure time dependence and spatial distribution induced by the shock wave are implemented in two different setups working simultaneously (Fig. 3). In the first case we use a continuous wave HeNe laser (10 mW,  $\lambda = 633$  nm, waist = 1 mm) to study the time-dependent change of the reflectivity (and thus refractive index) with nanosecond resolution [6]. As the surface plasmon resonance width is about 1 mrad ( $1^\circ$ )

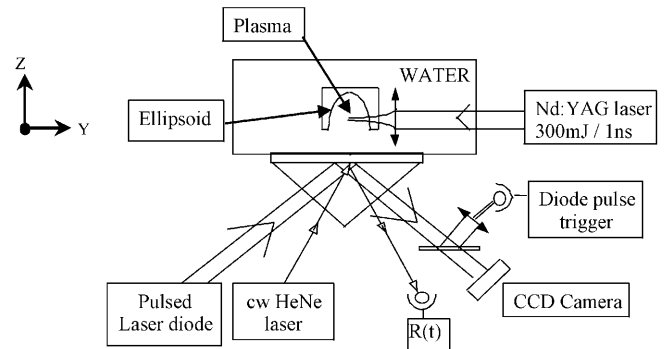


**Fig. 3.** Experimental setup for ns time-resolved lateral pressure distribution. A pulsed Nd:YAG laser is focused in water to create a plasma and to generate a shock wave which is focused on the metal film of the surface plasmon setup with an ellipsoidal mirror. The temporal reflectivity evolution  $R(t)$  of a cw He:Ne laser on the surface plasmon setup is detected in order to trace the pressure-time dependence  $P(t)$ . The image of the lateral distribution of the pressure wave is obtained by recording the lateral reflectivity  $R(x, y)$  pressure-induced modulation of a pulsed laser diode ( $S = 1 \text{ cm}^2$ ) on the surface plasmon setup. The diode pulse is triggered on the cw He:Ne signal with a delay line to choose the instant at which the picture is recorded

the laser divergence is limited to this value, which is of the order of magnitude of normal laser beam divergence: it does not require any specific optics. In order to avoid grazing laser incidence we used a high refractive index glass prism in the experiments. In the second setup plasmon microscopy [7] is used to determine the lateral pressure distribution at any time of the pressure evolution. For that purpose a pulsed laser diode (FWHM 15 ns,  $\lambda = 910$  nm) is used for the illumination of an area of  $1 \times 1 \text{ cm}^2$ . The pulsed laser diode is triggered by a delay line with respect to the shock wave generation (Nd:YAG laser pulse) in order to control the image time reference. Its reflected intensity on the prism is recorded with a normal low-cost CCD camera.

In order to get an intense shock wave a frequency-doubled Nd:YAG laser (FWHM 7 ns,  $\lambda = 532$  nm) is focused into a cell filled with water. At this point a plasma is generated which induces shock waves [11]. An additional enhancement of the pressure amplitudes is achieved by an ellipsoidal mirror. The measurements are performed at the second focal point of this mirror, which coincides with the silver film surface. At present, only one picture can be taken from each shock wave.

Each image of the spatial distribution of the induced pressure amplitude corresponds to a different single shock wave. Therefore the images corresponding to a different time delay can be compared quantitatively only if the shock wave reproducibility is sufficient. As the generated shock wave amplitude depends on the plasma expansion and as this strongly non-linear process is very sensitive to very small impurity concentrations [12], we compared the time-resolved reflectivity traces to check the shock wave reproducibility, which is a good approximation, although this signal is space averaged.

## 3 Results

With this setup we obtained pictures of a shock wave (generated with a laser Nd:YAG induced by optical breakdown in water) with ns time resolution and 50  $\mu\text{m}$  lateral resolution.

Such images can be seen in the sequence of three pictures (Fig. 4) with the time-dependent HeNe reflectivity signal  $R(t)$  corresponding to each incident shock wave. From the HeNe signal, the positive pressure peak can be estimated to be 10 MPa (100 atm). We also observed a small tensile negative pressure variation. The central part of the shock wave signal corresponds to a delay time of about 34.5  $\mu\text{s}$ , which is the time needed for the shock wave to propagate from the plasma region to the silver surface.

The pictures shown represent the lateral distribution of the pressure recorded with the CCD camera at the time delay indicated with an arrow on each corresponding HeNe time reflectivity  $R(t)$  signal. The lateral resolution of these pictures is about 50  $\mu\text{m}$  without any specific viewing optics. It can be easily optimized and increased by a factor of 5 to 10 with the use of an appropriate telescope objective. The grayscale intensity (from completely black to maximum white intensity) of these pictures gives a linear pressure scale directly (with respect to the surface plasmon resonance at the diode laser wavelength). Each pixel intensity is directly proportional to the local pressure variation (which can be positive or negative and is shown to be higher than estimated by the time-resolved and space-averaged data). Image (a) corresponds to the acoustic wave arrival ( $t = 34.20 \mu\text{s}$ ). Image (b) corresponds to the HeNe maximum positive pressure peak amplitude ( $t = 34.40 \mu\text{s}$ ). Image (c) corresponds to the HeNe negative pressure peak amplitude ( $t = 34.50 \mu\text{s}$ ).

In pictures (a), (b), and (c) (providing time evolution of the pressure lateral distribution) one can clearly observe two bright half circles which represent the two maximum pressure lobes propagating in the  $y$ -direction and crossing at the instant of image (b). For a punctual plasma source we should

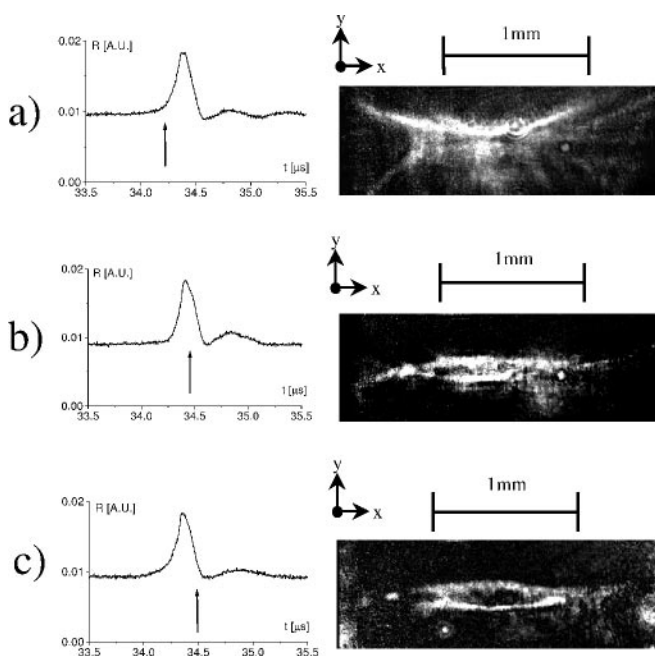


**Fig. 4a–c.** Pressure-time evolution from cw He:Ne reflectivity  $R(t)$  and lateral pressure distribution images recorded with a CCD camera from the pulsed laser diode reflectivity  $R(x, y)$ . The sequence **a**, **b**, and **c** shows  $R(t)$  and  $R(x, y)$  for different time delays of the diode laser pulse with respect to shock wave generation. In the shock wave images the maximum local pressure is not the same as in the He:Ne pressure estimate ( $R(t)$  maximum is 20 MPa)

observe only one bright circle. The observed pressure image is more complex but it can be easily understood if the expanding plasma geometry which generates the shock waves (before focusing on the prism surface) is an ellipsoid with main axes oriented in the  $y$ -direction. Then the spatial distribution of the focused acoustic wave is no longer spherical but elliptical (the image of the source geometry after focusing). In fact, this is the real situation, as the Nd:YAG laser which is focused in water to produce the plasma is a gaussian beam propagating in the  $y$ -direction. It is well known that the shape of the plasma produced is an ellipsoid oriented in the laser propagating direction [11, 12].

The best sensitivity achieved with the time-resolved reflectivity (cw He:Ne signal) is about  $\Delta R/R = 1\%$ . It is only imposed by the amplitude noise of the laser and by the noise of the fast photodiode used. We obtained the best sensitivity to pressure with 53 nm Ag film thickness (which corresponds to the surface plasmon resonance with optimized half width in water). With this plasmon resonance the reflectivity modulation  $\Delta R/R$  attains its maximum (100%) for 20 MPa pressure modulation. By decreasing the silver film thickness (or using gold, which has a broad surface plasmon resonance), it is possible to broaden the surface plasmon resonance ( $\Delta\theta_{1/2}$ ) and to increase the high-pressure range, but of course in this case the pressure sensitivity decreases. The sensitivity of these first lateral pressure images with ns time resolution can be enhanced by the use of a more sensitive CCD camera or with a bigger pulse laser fluence.

This optical sensor for acoustic waves provides a very suitable tool for obtaining quantitative results on the early stage of bubble nucleation at a liquid-solid interface [13] (induced by either laser shot or ultrasonics) as it requires a local probe technique achieving good pressure sensitivity with both time (bubble dynamic in ns range) and spatial resolutions (bubble size about  $\mu\text{m}$ ). However, the idea of an optical acoustic sensor is not restricted to surface plasmon waves. In this way we have started to provide an optical waveguide acoustic sensor using the optical path modulation induced by a traveling acoustic wave through it [14].

## 4 Conclusion

We have performed the first portable optical imaging sensor for acoustic waves with both ns and  $\mu\text{m}$  resolution in the pressure range from 0.2 to 20 MPa. The main advantage of this time-resolved pressure distribution imaging technique is its high sensitivity to small variations of the index of refraction in the low-pressure regime. Actually this is the only technique able to show the lateral structure of the tensile acoustic pressure (negative) which is much more intense than the estimated space-averaged pressure due to its lateral structure.

As the laser probe reflectivity dependence is linear with the pressure, this sensor provides the time-resolved pressure spatial evolution directly. Because this property, after absolute pressure calibration with a well-known static pressure applied, one can get a portable calibrated acoustic wave imaging technique with both ns time resolution and few  $\mu\text{m}$  spatial resolution.

As mentioned above, this new sensor technique can be applied to control the laser ablation or laser cleaning processes as well as medical shock wave techniques online, and to study

the early stage of laser-induced bubble nucleation at the solid-liquid interface, which is used in steam laser cleaning and in ultrasonic cleaning methods.

## References

1. H.D. Sussner, A. Michals, S. Asstalg, S. Hunkfinger, K. Dransfeld: Phys. Lett. A **45**(6), 475 (1973)
2. J. Staudenraus, W. Eizenmenger: Ultrasonics **31**(4), 267 (1993)
3. W. Knoll: Mater. Res. Soc. Bulletin **XVI**, 29 (1991)
4. A.C. Tam: Rev. Mod. Phys. **58**(2), 381 (1984)
5. J.A. Parrish, T. Deutsch: IEEE J. Quantum Electron **QE-20**, 1386 (1984)
6. A. Schilling, O. Yavas, J. Bischof, J. Boneberg, P. Leiderer: Appl. Phys. Lett. **69**(27), 4159 (1996)
7. S. Herminghaus, C. Bechinger, W. Peterson, P. Leiderer: Opt. Commun. **112**, 16 (1994)
8. E. Kretschmann, H. Raether: Z. Naturf. A **32**, 2135 (1968)
9. H.S. Yadav, D.S. Murthy, S.N. Verma, K.H.C. Sinha, B.M. Gupta, D. Chand: J. Appl. Phys. **44**(5), 2197 (1973)
10. H. Raether: *Surface Plasmons on Smooth and Rough Surfaces and on Gratings* (Springer, Berlin, Heidelberg 1988)
11. J. Noack, D.X. Hammer, G.D. Noojin, B.A. Rockwell, A. Vogel: J. Appl. Phys. **83**(12), 7488 (1998)
12. F.J. Scherbaum, R. Knopp, J.I. Kim: Appl. Phys. B **63**, 299 (1996)
13. O. Yavas, A. Schilling, J. Bischof, J. Boneberg, P. Leiderer: Appl. Phys. A **64**, 331 (1997)
14. S. Herminghaus, P. Leiderer: Appl. Phys. Lett. **54**(2), 99 (1989)